EVALUATION OF DESIGN CONCEPTS FOR HOLES IN GLULAM BEAMS — COMPARISON WITH TEST RESULTS

EVALUIERUNG VON BEMESSUNGSANSÄTZEN FÜR DURCHBRÜCHE IN BRETTSCHICHTHOLZ — ABGLEICH MIT VERSUCHSERGEBNISSEN

Cristóbal Tapia, Simon Aicher

Materials Testing Institute (MPA), University of Stuttgart, Otto-Graf-Institute

SUMMARY

Holes with round or rectangular shapes in monolithic glued laminated timber (GLT) beams represent a frequent construction necessity. The holes disturb the stress flow within the beam, resulting in stress concentration areas at the periphery of the hole. The holes cause stresses perpendicular to the grain, previously not existing, but also shear and normal stress concentrations depending on the shape, size and placement of the opening. The basic mechanics of the load and stress redistribution in the orthotropic, or better said, cylindrical anisotropic material wood are well understood. This applies to the material resistance, too, which has to account for the stochastic defect distribution within the timber.

So far, the European timber design code, Eurocode 5 (EC5), does not contain any provisions for holes in GLT. Contrary hereto, the German National Annex to EC5 and North American AITC provisions specify design rules for unreinforced holes. The present German national rules have proven to provide a safe design of holes. However, the approach and especially the related constructive detailing can be regraded in part overly conservative (e.g. related to the moment influence and permissible hole size). Apart from various modelling approaches and few design provisions, several extensive tests series with structural-sized GLT beams with holes of different sizes and shapes have been performed in the last two decades, providing sufficient test data for the model calibration.

This paper reports on two rather new elaborate design approaches for holes in GLT. One of the methods enables a formally equal design of round and rectangular holes. Both design methods are shortly described and then compared with each other and, more important, with reported test results. Further, a comparison with the current German design provisions is included.

ZUSAMMENFASSUNG

Durchbrüche mit runder oder rechteckiger Berandung in Brettschichtholz (BSH)-Trägern repräsentieren eine häufige konstruktive Notwendigkeit. Die Durchbrüche stören den Spannungsfluss in Trägern und erzeugen Spannungskonzentrationsbereiche an der Durchbruchsberandung. Ein Durchbruch erzeugt Spannungen rechtwinklig zur Faserrichtung, die ausschließlich aus der Lastumlagerung resultieren, aber auch Schub- und Normalspannungserhöhungen/konzentrationen, die ausgeprägt von der Form, der Größe und der Anordnung des Durchbruches abhängen. Die grundlegende Mechanik der Last- bzw. Spannungsumlagerung in dem orthotropen oder genauer, zylindrisch anisotropen Material Holz ist wohl verstanden. Die gilt ebenso für den Materialwiderstand, der die stochastische Defektverteilung zu berücksichtigen hat.

Zum heutigen Zeitpunkt enthält die europäische Holzbau-Bemessungsnorm Eurocode 5 (EC5) keine Bemessungsregeln für Durchbrüche. Im Gegensatz hierzu enthalten der deutsche nationale Anhang zum EC5 und US-amerikanische AITC Dokument Nachweise für unverstärkte BSH-Durchbrüche. Die heutigen deutschen Bemessungsregeln haben nachweislich zu einer sicheren Bemessung von Durchbrüchen geführt, wobei der Nachweis und insbesondere die damit verbundenen konstruktiven Ausführungsregeln teilweise als übermäßig konservativ anzusehen sind (z.B. bezüglich des Momenteinflusses und der zulässigen Durchbruchsgrößen). Neben diversen Modellierungsansätzen und wenigen Bemessungsregeln wurden in den beiden letzten Jahrzehnten einige umfangreiche Versuchsreihen mit voll maßstäblichen BSH-Trägern mit Durchbrüchen unterschiedlicher Größe und Durchbruchsberandung durchgeführt.

Dieser Aufsatz berichtet über zwei vergleichsweise neue, sehr detaillierte Bemessungsansätze für Durchbrüche in Brettschichtholz, wobei ein Vorschlag eine formal gleiche Bemessung von runden und rechteckigen Durchbrüchen ermöglicht. Beide Bemessungsvorschläge werden erläutert und sodann miteinander und, wichtiger, mit literaturbekannten Versuchsreihen verglichen. Diesbezüglich ist auch ein Vergleich mit dem heutigen deutschen Bemessungsansatz beinhaltet.

KEYWORDS: Glued laminated timber (GLT), unreinforced holes, calculation method, design codes, Eurocode 5, test results

1. INTRODUCTION

The placement of holes in glued laminated timber (GLT) beams is a common design aspect in timber structures. Holes are required mostly for the passing-through of diverse infrastructure systems, such as heating, sanitary or electrical installations. Although the use of larger holes in GLT elements should, in a first consideration, be avoided, there are many situations where this is not possible, mainly due to architectonic or economic restrictions.

Under typical loading conditions of beams, moment and shear forces will be present in the region containing the hole. Owed to the geometric discontinuity introduced by the hole a redistribution of stresses occurs in the vicinity of the hole, re-routing shear and bending stresses around the hole. This process inevitably leads to high stress concentrations perpendicular to the fiber at the immediate vicinity of the hole, coincidentally being this the direction of lowest material resistance of wood and hence of GLT. Further, and especially in the case of rectangular holes, shear stresses peaks occur at the corners. For the case of larger holes with openings beyond about 40% of the beam depth, the bending normal stresses reveal stress peaks at the hole periphery, deviating significantly from the elementary beam theory. This stress interaction facilitates the initiation and propagation of cracks in the affected region, possibly leading to a major and possibly global failure of the element.

The current generation of Eurocode 5 (EC5) does not contain provisions for the design of holes in GLT beams, however, rules are provided in some national EC5 annex documents. The German National Annex (DIN EN 1995-1-1/NA [8]) contains an elaborated design concept based on the computation of virtual tensile forces, $F_{t,90}$, resulting from the integration of the tensile stresses perpendicular to the fiber in the vicinity of the hole [4, 3]. This force $F_{t,90}$ is composed of two additive terms, $F_{t,90,M}$ and $F_{t,90,V}$, corresponding to the contributions due to moment and shear force, respectively.

By means of numerical analysis Aicher et al. [3] found that the term associated to the moment contribution, $F_{t,90,M}$, in the form presented in DIN EN 1995-1-1/NA [8], leads to highly conservative results, and derived a new, more appropriate equation for this term. Recently, Tapia and Aicher [15] proposed a new set of design equations based on a parametric FE analysis. These equations were developed to work for both, round and rectangular holes placed at the beam mid-depth. At the same time, Danzer et al. [7] presented a different set of design equations, explicitly considering the eccentricity of the holes. These equations were developed exclusively for round holes. In [7] a comparison was performed with both, literature-reported and own [7] experimental results, showing an overall rather good agreement with the results presented by Aicher et al. [3] and own experiments.

This article is a contribution to the ongoing efforts in providing design provisions for holes in GLT beams for the new Eurocode 5. For this, a comparison of the equations presented by Danzer et al. [7] and Tapia and Aicher [15] will be compared to experimental results reported in the literature, as well as with the current provisions from DIN EN 1995-1-1/NA [8].

2. GENERAL CONSIDERATIONS REGARDING THE DESIGN OF HOLES IN GLULAM

The design of unreinforced holes in GLT gravitates around the concept of a fictive resultant tensile force, $F_{t,90}$, representing the integral of the stresses perpendicular to the grain ($\sigma_{t,90}$) in the hole vicinity, along the path of most probable crack propagation. Fig. 1 illustrates this concept using a round hole as example. Regions 1 and 2 correspond to the zones affected by the tensile stresses $\sigma_{t,90}$, as depicted by the lighter (yellowish) colors.

If a horizontal path is defined starting at the position of maximum $\sigma_{t,90}$, occurring at an angle φ_1, the stresses $\sigma_{t,90}$ along this path will decline with increasing distance to the stress disturbance as shown in the Fig. 1 (right), until $\sigma_{t,90} = 0$ is reached at $x = \ell_{t,90}$. The integral of this stresses throughout the length $\ell_{t,90}$ and width, b, of the cross-section, results in the vertical tensile force $F_{t,90}$. It can be shown [3, 15] that this force is the additive result of two components. One component, $F_{t,90,V}$, stems from the redistribution of shear stresses around the hole, whilst $F_{t,90,M}$ is attributed to the redistribution of the bending stresses due to the presence of the hole.

Since the force $F_{t,90}$ can be decomposed into the terms $F_{t,90,V}$ and $F_{t,90,M}$, specific integration lengths for each of these forces can be considered, too. These integration lengths are called $\ell_{t,90,V}$ and $\ell_{t,90,M}$, respectively. The integration length $\ell_{t,90}$ of the force $F_{t,90}$ is then also used for the computation of the virtual capacity $R_{t,90}$

that will *resist* the action of $F_{t,90}$ (more details in Section 3). The design approaches presented in the following section consider equations to estimate both, $F_{t,90}$ and the corresponding resisting force.

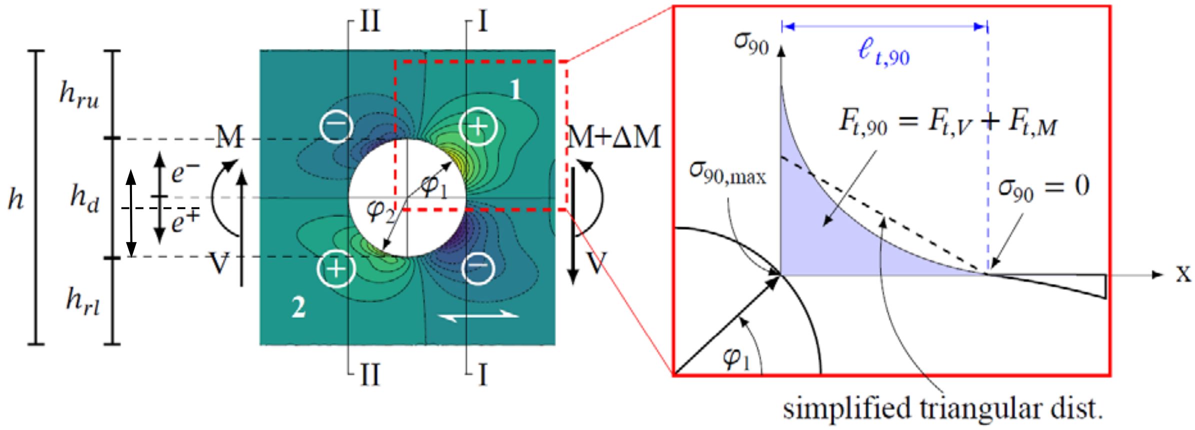

Fig 1: Definition of tensile force and integration length. Dimensions according to DIN EN 1995-1-1/NA [8]

3. DESIGN APPROACHES

3.1 GERMAN NATIONAL ANNEX TO EC5

The present design provisions for round and rectangular holes given in require the following relation to be satisfied:

$$\frac{F_{t,90,d}}{R_{t,90,d}} = \frac{F_{t,90,V,d} + F_{t,90,M,d}}{0{,}5 \cdot \ell_{t,90} \cdot b \cdot k_{t,90} \cdot f_{t,90,d}} \leq 1{,}0 \qquad (1)$$

where $f_{t,90,d}$ is the design value of the tensile strength in the direction perpendicular to the fiber, based on the characteristic (5%-quantile) strength $f_{t,90,k}$ and b is the width of the beam. The factor 0,5 considers an approximated triangular stress distribution along the probable crack-surface, certainly underestimating the peak stresses (see Fig. 1 right). The term $k_{t,90}$ is a factor that accounts for the pronounced size effect (here assumed to result exclusively from the beam depth) of the GLT element as

$$k_{t,90} = \min\left\{1; \left(\frac{450}{h}\right)^{0,5}\right\}, \tag{2}$$

where h is the depth of the beam. (Note: The specified size effect corresponds to a linear elastic fracture mechanics (LEFM) size influence, then deduced from the results by Höfflin and Aicher [12].) The length $\ell_{t,90}$ is computed differently for round and rectangular holes as

$$\ell_{t,90} = \begin{cases} 0{,}353 \cdot h_d + 0{,}5 \cdot h & \text{, for round holes} \\ 0{,}5 \cdot (h_d + h) & \text{, for rectangular holes.} \end{cases} \tag{3}$$

Finally, the two components of the force $F_{t,90,d}$ are estimated by means of the following equations (in the following, the index d related to the design load level is omitted):

$$F_{t,90,V} = \frac{V \cdot h_d}{4 \cdot h} \cdot \left(3 - \frac{h_d^2}{h^2}\right) \tag{4}$$

$$F_{t,90.M} = 0{,}008 \cdot \frac{M}{h_r}, \tag{5}$$

where $h_r = \min\{h_{ru}; h_{rl}\}$. Further, for the case of round holes h_d may be multiplied by the factor 0,7. The dimensional notations for round holes according to DIN EN 1995-1-1/NA [8] are shown in Fig. 1, where the definition for the positive and negative eccentricity directions are given, too.

3.2 DESIGN CONCEPT BY DANZER ET AL.

Danzer et al. [7] proposed a design concept for round holes based on almost the same scheme as currently given in DIN EN 1995-1-1/NA [8]. However, Eq. (1) is slightly modified to include the individual integration lengths of each $F_{t,90}$ component resulting from V and M as

$$\frac{\frac{F_{t,90,V}}{\ell_{t,90,V}}+\frac{F_{t,90,M}}{\ell_{t,90,M}}}{0{,}5\cdot b\cdot f_{t,90,k}\cdot k_{\mathrm{vol}}}\leq 1.0; \tag{6}$$

where

$$F_{t,90,V}=\frac{V\cdot 0{,}7\cdot h_d}{4\cdot h}\cdot\left(3-\left(\frac{0{,}7\cdot h_d}{h}\right)^2\right)\cdot k_{\mathrm{ecc}} \tag{7}$$

$$k_{\mathrm{ecc}}=0{,}1+\frac{h_d}{h}+4{,}5\cdot\frac{h_r}{h}+0{,}2\cdot\frac{h_d\cdot h_r}{h^2}-4{,}9\cdot\left(\frac{h_r}{h}\right)^2 \tag{8}$$

$$\ell_{t,90,V}=1{,}3\cdot h_d \tag{9}$$

and

$$F_{t,90,M,1}=M\cdot\frac{h_d}{h^3}\cdot\max\begin{Bmatrix}-0{,}62\cdot(e-0{,}13\cdot h_d)\\ -0{,}2\cdot(e-0{,}45\cdot h_d)\\ 0{,}3\cdot(e-0{,}08\cdot h_d)\end{Bmatrix} \tag{10}$$

$$\ell_{t,90,M,1}=0{,}8\cdot h_d\cdot\left(1-\frac{e}{h_d}\right) \tag{11}$$

$$F_{t,90,M,2}=M\cdot\frac{h_d}{h^3}\cdot 0{,}22\cdot(e+0{,}19\cdot h_d) \tag{12}$$

$$\ell_{t,90,M,2}=0{,}4\cdot h_d. \tag{13}$$

Different from [8], the size effect is now represented as a volume effect, k_{vol}, similar as in other design problems, where tensile strength perpendicular to the grain is a decisive factor (e.g. curved and tapered GLT beams). Considering a standard reference volume of $V_0 = 0{,}01\ \mathrm{m}^3$, k_{vol} is computed as

$$k_{\mathrm{vol}}=\left(\frac{V_0}{0{,}225\cdot b\cdot h_d^2}\right)^{0{,}2}. \tag{14}$$

As it can be noticed, the vertical eccentricity e of the holes is explicitly considered by the factors k_{ecc}, h_r and e in the equations (7), (8), (10)-(12). In contrast, the German National Annex to EC5 only considers this (in a very crude form) in the moment component (see Eq. (5)).

For details regarding the derivation of the above equations the reader is referred to [7]. It is, however, relevant to mention that the k_{vol} factor was derived by means of a Weibull analysis on an FE model, following the concepts presented by Höf-flin and Aicher [12]. At that time a very similar value for k_{vol} was derived, with a factor 0,19 instead of 0,225 in the denominator.

3.3 NEW DESIGN CONCEPT

The here proposed design concept for unreinforced holes is based on the equations for $F_{t,90}$ presented by Tapia and Aicher [15]. These were derived by means of a parametric analysis on the basis of an FE model with holes of different shapes and relative sizes, including circular, as well as rectangular holes with side aspect ratios a/h_d of 1,0 and 2,5 ($a =$ hole length parallel to beam axis). A vertically centered placement of the holes was considered, i.e. no eccentricities.

In this particular case no Weibull integration of the fracture-relevant stresses $\sigma_{t,90}$ was done, as opposed to the approach in [7]. The impact of the stochastically distributed material defects within the differently shaped stress fields, is exclusively accounted for by the volume factor on the resistance side. The virtual tensile forces for a fictive *pure shear* condition and pure moment were derived as

$$F_{t,90,V} = \frac{V \cdot \xi h_d}{4h} \cdot \left[3 - \left(\frac{\xi h_d}{h}\right)^2\right] \cdot \left[1 + \alpha\left(\frac{\xi h_d}{h}\right)\right] \tag{15}$$

$$F_{t,90,M} = \frac{0{,}1 \cdot M}{h} \cdot \left(\frac{\xi h_d}{h}\right)^2 \cdot \left[1 + \kappa\left(\frac{\xi h_d}{h}\right)\right] \tag{16}$$

where the parameters ξ, α and κ, which depend on the shape of the hole, are specified in Table 1. For side aspect ratios a/h_d of rectangular holes between 1 and 2,5 linear interpolation shall be used.

Eqs. (15) and (16) are used with Eq. (6) for the design verification of the hole, where the integration lengths $\ell_{t,90,V}$ as well as the factor k_{vol} are adopted from Danzer et al. [7], here given in Eqs. (9) and (14).

Table 1: Paramters to be used in Eqs. (15) and (16) accounting for different hole shapes

Shape	ξ	α	κ
Round	0,81	0,43	0,40
Rect. (1:1)	0,84	1,1	0,16
Rect. (2,5:1)	0,86	1,9	0,33

Verifying computations revealed overall marginal differences. However, the integration length $\ell_{t,90,M}$, related to the $\sigma_{t,90}$ redistribution as a result of the moment action is taken somewhat different as

$$\ell_{\mathrm{t,90,M}} = 0{,}5 \cdot h_d \tag{17}$$

based on results from finite element computations performed in the context of this paper. It should be noted that a rather similar expression has been obtained previously by Aicher and Höfflin [1].

Although Eqs. (15) and (16) do not consider a possible eccentricity of the holes, it was shown numerically [15] that for small eccentricities and moment-to-shear-force ratios (M/V) between 1,5 h and 5 h, the error incurred is rather small.

4. LITERATURE-REPORTED EXPERIMENTAL DATA

The scientific literature presents a significant number of experimental campaigns on unreinforced holes in GLT beams. During the 1970's and 1980's substantial contributions were presented i.a. by Frech and Kolb [11] (however mostly on reinforced holes), Johannesson [13] and Pentalla [14], both for circular and rectangular holes. Later, experimental campaigns were published by Aicher and Höfflin [2], Danielsson [5] and Danzer et al. [6]. The last three datasets, well documented with regard to all material parameters, are used here to assess the adequacy of the design provisions according to the three models presented in Section 3.

The first dataset [2] consists of a total of eleven test series, each of them comprising five specimens. The holes had round shapes of relative sizes $h_d/h = 0{,}2$, 0,3 and 0,4, and the beam depths, differing by a factor of two, were h = 455 mm and 900 mm. Two M/V ratios were investigated (1,5 and 5,9). Details can be taken from Table 2.

Table 2: Test configurations and 5%-quantiles of test and different design approaches

		N	hole shape	h_d/h [-]	e/h [-]	h [mm]	b [mm]	M/V [h]	5%-quantiles: test results $V_{\mathrm{exp},k}$ 5Q1 [kN]	5Q2 [kN]	design approach $V_{\mathrm{calc},k}$ D1 [kN]	D2 [kN]	D3 [kN]
1	Aicher and Höfflin [2]	5	round	0,20	0	450	120	1,5	46,9	53,8	52,6	51,0	43,3
2		6	round	0,30	0	450	120	1,5	49,1	52,6	41,8	40,7	32,5
3		4	round	0,40	0	450	120	1,5	29,3	34,4	35,0	34,8	26,9
4		5	round	0,20	0	900	120	1,5	57,0	67,7	79,7	77,4	61,3
5		6	round	0,30	0	900	120	1,5	72,2	77,5	63,4	61,7	46,0
6		5	round	0,40	0	900	120	1,5	50,6	55,2	53,1	52,8	38,0
7		5	round	0,30	0	450	120	5	43,3	47,0	33,1	34,0	25,4
8		6	round	0,40	0	450	120	5	34,3	37,3	26,2	27,9	21,7
9		4	round	0,20	0	900	120	5	72,8	82,8	67,5	67,9	44,9
10		5	round	0,30	0	900	120	5	37,9	42,1	50,2	51,6	35,9
11		5	round	0,40	0	900	120	5	29,9	36,4	39,7	42,2	30,6
12	Danzer et al. [6]	3	round	0,25	-0,175	400	120	1,5	46,7	54,0	43,3	40,0	29,6
13		3	round	0,25	-0,100	400	120	1,5	43,2	48,3	43,3	40,2	31,3
14		3	round	0,25	0,100	400	120	1,5	38,2	44,4	43,3	39,7	33,8
15		3	round	0,25	0,175	400	120	1,5	50,4	56,8	43,3	37,2	34,3
16		3	round	0,35	-0,175	400	120	1,5	41,5	49,8	35,5	35,4	23,5
17		3	round	0,35	-0,100	400	120	1,5	45,0	48,9	35,5	34,7	24,9
18		3	round	0,35	0,100	400	120	1,5	41,2	46,8	35,5	33,2	26,7
19		3	round	0,35	0,175	400	120	1,5	35,3	41,2	35,5	30,5	27,1
20	Danielsson [5]	8	rect 1)	0,33	0	630	120	2	40,6	43,0	37,8	–	34,9
21		4	rect	0,33	0	630	120	0	54,4	56,9	43,8	–	41,7
22		4	rect	0,33	0	180	120	2	20,7	22,2	17,8	–	11,8
23		4	rect	0,33	0	180	120	0	22,2	23,6	20,6	–	14,1

5Q1: 5%-quant. acc. to EN 14358 [9]
5Q2: 5%-quant. with modified k_s value acc. 14454 [10]
D1: here proposed design concept
D2: design concept proposed by Danzer et al. [7]
D3: design acc. to DIN EN 1995-1-1/NA [8]
M/V: moment-to-shear-force ratios, *M/V*, at hole center
1): side aspect ratio 1:1

The results reported by Danielsson [5] comprise a total of five series, each with four specimens. (Two series only differed in the type of build-up-one homogeneous, the other combined-reason for which they are treated here as one series with eight specimens.) Only quadratic-shaped holes (side aspect ratio $a : h_d = 1 : 1$) of relative size $h_d/h = 0{,}33$ were considered. Two cross-sectional depths of 180 mm and 630 mm were studied, as well as two M/V ratios of 0,0 and 2,0 (see Table 2). Both, this and the previous dataset [2] consider exclusively holes placed at mid-depth (symmetrical arrangement).

The third dataset with results from [6] presents circular holes placed eccentrically, with eccentricity ratios $\frac{e}{h} = \pm\, 0{,}1$ and ± 0,175, respectively. Two h_d/h ratios of

0,25 and 0,35 were used, where the beam depth was 400 mm throughout. The ratio M/V was kept constant at 1,5 (see Table 2).

To sum up, the test results comprise 23 different tests series with 99 individual specimens in total, where the number of specimens per series ranges between three and eight. The GLT strength classes comprise GL20 to GL32.

5. EXPERIMENTAL RESULTS VERSUS DESIGN APPROACHES

5.1 COMPARISON BETWEEN BOTH NEW DESIGN CONCEPTS

The above sketched design concepts are compared to the cited literature-reported experimental results. The following abbreviations are used to differentiate between the different approaches: *D1* is the design concept presented by the authors here (see Section 3.3); *D2* corresponds to the design concept by Danzer et al. [7]; and *D3* represents the design specified in DIN EN 1995-1-1/NA [8]. The comparison is given in a dimensionless format as ratio of the calculated characteristic (5%-quantile) shear force capacity vs. the experimental characteristic value of the respective test series, $V_{\text{calc},k}/V_{\text{exp},k}$. The comparison is further performed on the level of the individual specimens per test series with the ratio $V_{\text{calc},k}/V_{\text{exp},i}$.

The calculation of the characteristic shear-force capacity, $V_{\text{exp},k}$, of the individual test series was performed with two different methods. In the first approach, here denoted as 5Q1, the true number of specimens per series was used to derive the 5%-quantile value according to EN 14358 [9] assuming a lognormal distribution. This approach leads to partially extremely low characteristic values, due to the very low number of specimens per test series, then resulting in a statistical k_s factor in the range of 2,3 up to 3,2 for each respective test series. A more realistic evaluation of the 5%-quantile for the individual test series was performed by determining a global coefficient of variation considering each individual test result according to EN 14454 [10]. This method, also employed by Danzer et al. [7], delivers a k_s value of 1,76, being almost identical to the value used in [7]. The shear force ratios are given in graphical manner in Figs. 2a and 2b, for both reported methods of 5%-quantile determination, respectively. Table 2 contains the 5%-quantile values for the tests (5Q1 and 5Q2) and for the different design approaches (D1, D2 and D3), together with information of the test configurations.

Shear force ratios < 1 characterize the conservative, i.e. the safe side. First the shear force ratios of the individual test results, $V_{\text{calc},k}/V_{\text{exp},i}$, are commented. (Note: the ratios of the individual values remain of course unchanged in both Figures 2a, b.) It can be observed from either Fig. 2a or 2b that most ratios for the individual specimens are conservative, with the exception of some results from test series 10 and 11, which deliver ratios up to 14% above 1. The non-conservative results are related to test series with large round holes, which showed a rather high scatter denoted by a coefficient of variation (COV) of 24%. Noteworthy, the previous finding is valid for both calculation models D1 and D2.

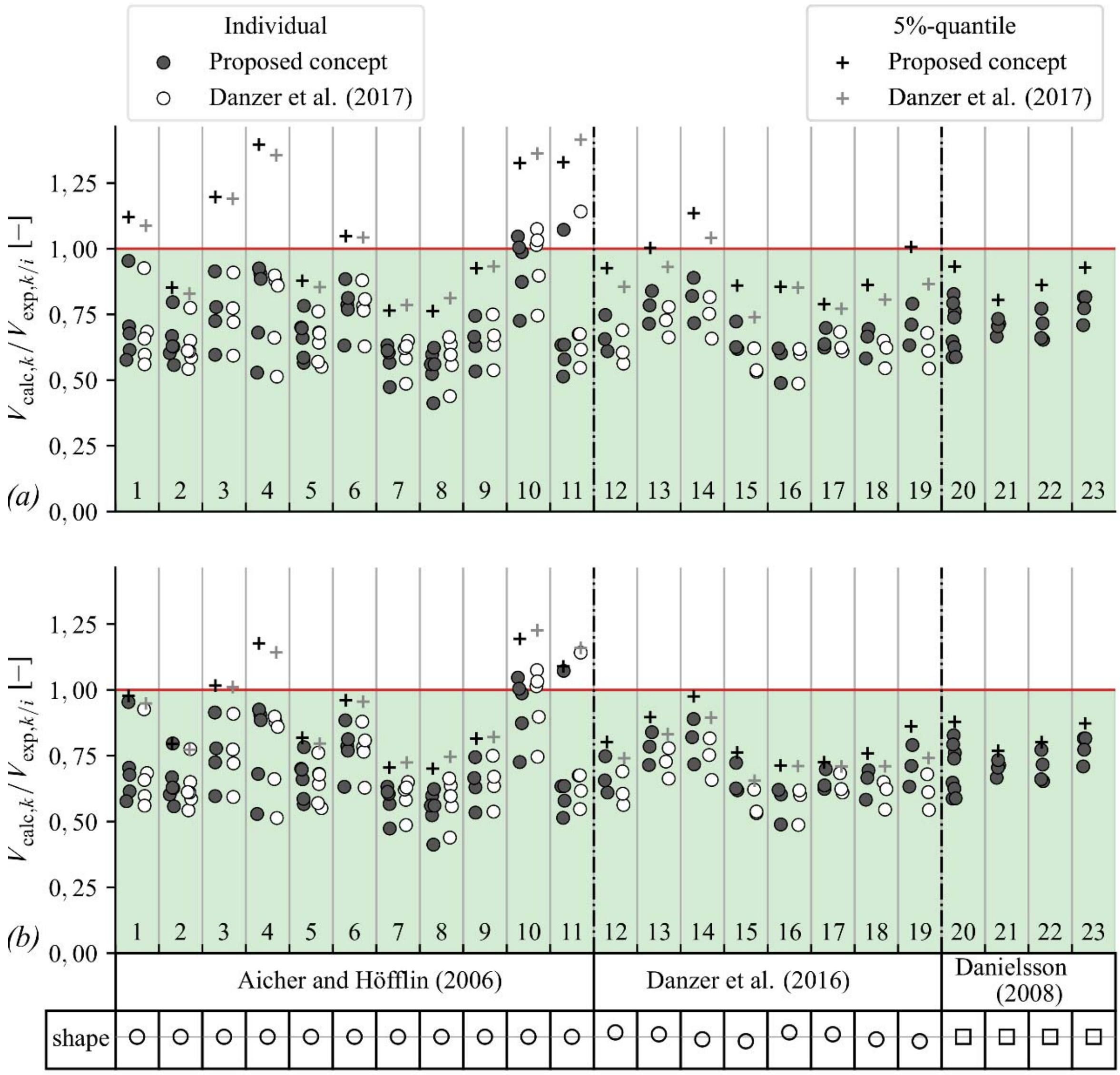

Fig. 2: Comparison of design concept D1 with D2 for literature-reported data. Characteristic (5%-quantile) values computed (a) according to EN 14358 [9] accounting for specimen number per individual test series, and (b) with k_s = 1,76 derived according to EN 14454 [10]

As a general trend, it can be seen that both design concepts give similar results (see Table 2), however the results obtained by the model D2 are in general lower and hence slightly more conservative as the test results. In average, $V_{D2,k} / V_{D1,k} = 0{,}97 \pm 0{,}05$. The differences between both models related to D1 are in the range of -14% and +6%, respectively.

Regarding the shear force ratios based on the characteristic values of both, calculation and test results, $V_{\text{calc},k}/V_{\text{exp},k}$, significant differences can be observed depending on the method used to calculate $V_{\text{exp},k}$. For the case where $V_{\text{exp},k}$ is based strictly on EN 14358 [9] (Fig. 2a) the ratios for seven of the total of 23 test series fall above 1, showing values between 1,1 and 1,4; this is true for both models D1 and D2. All other ratios are either equal or (significantly) below unity. All conservative shear force ratios are related to tests series with little scatter.

Regarding the more sensible comparison of the characteristic design and test results based on experimental characteristic values evaluated on the basis of all test results and hence with a factor $k_s = 1{,}76$ as given above, almost all ratios $V_{\text{calc},k}/V_{\text{exp},k}$ of both design approaches are on the conservative side (Fig. 2b). Only for four test series the ratios are higher (1% to 19%) than one (series 3, 4, 10 and 11).

5.2 COMPARISON WITH PROVISIONS OF GERMAN NATIONAL ANNEX TO EC5

Fig. 3 presents the results of model D1 compared to the results obtained according to DIN EN 1995-1-1/NA [8] (model D3), see also Table 2. (Note: characteristic values from tests based on EN 14454 [10].) It is evident that the current German design provisions deliver rather conservative results, in average moving at around 60% of the experimental failure loads. On the characteristic strength level, the ratio $V_{\text{D3},k}/V_{\text{exp},k}$ amounts in average to 0,66.

Three factors are influential for the pronounced differences with the test results. Firstly, there is a significant difference in the equations for the vertical tensile force $F_{t,90}$, as it is known [3] that the moment component $F_{t,90,M}$ is highly conservative (better said, it is wrong). Secondly, the size effect accounted by $k_{\text{t},90}$ is pronouncedly more severe in model D3, where a linear elastic fracture mechanics factor $\sqrt{h_{\text{ref}}/h}$ serves to capture the size influence. In this context, it is noteworthy that the results from 2D geometrically-scaled specimens with round holes reported in Aicher and Höfflin [2] delivered a rather pronounced size effect, despite the fact that no stress singularity or sharp corner is acting.

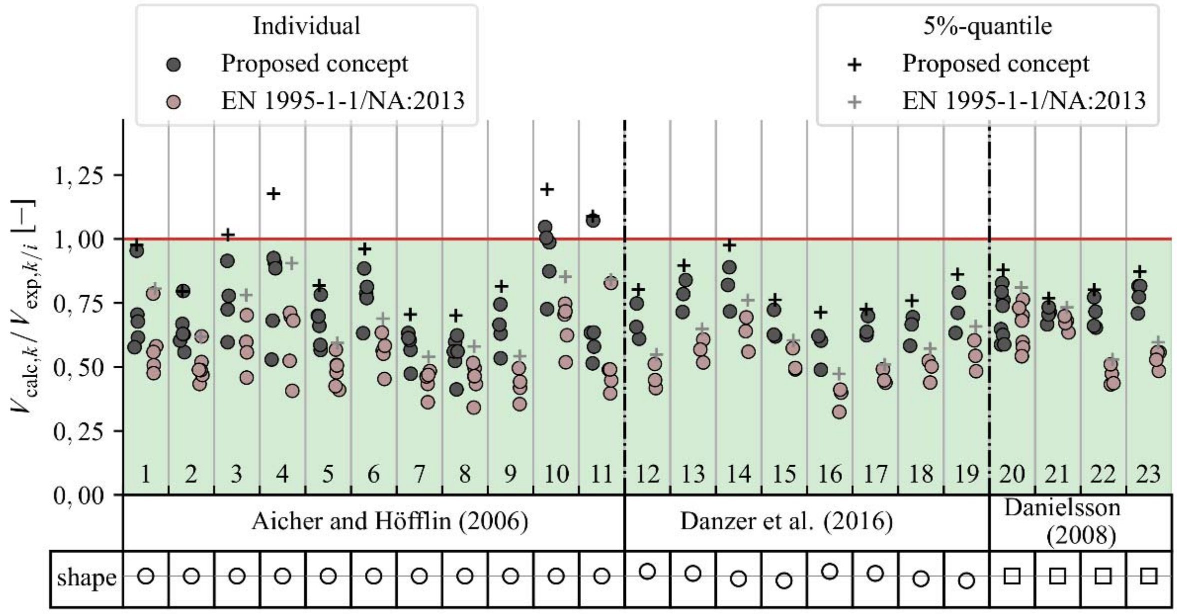

Fig. 3: Comparison of design concept D1 with D3 for literature-reported data. Characteristic (5%-quantile) values computed according to EN 14358 [9] with $k_s = 1{,}76$ *derived according to EN 14454 [10]*

6. CONCLUSIONS

The presented evaluations show that the newly proposed, transparent design approach of the authors leads to a conservative, yet still economic design of holes of different shapes in different sized glulam beams. This is further true for holes with small eccentricities, at least in regions with low moment-to-shear-force ratios. The latter is proven by the comparison with recently published results of tests with round holes, placed moderately eccentric with respect to the beam mid-depth.

REFERENCES

[1] AICHER, S., HÖFFLIN, L.: *Round holes in glulam members. Part 1: Analysis*. (in German). In: *Bautechnik* Vol. 78.10 (2001), pp 706-715

[2] AICHER, S., HÖFFLIN, L.: *Tragfähigkeit und Bemessung von Brettschichtholzträgern mit runden Durchbrüchen – Sicherheitsrelevante Modifikationen der Bemessungsverfahren nach Eurocode 5 und DIN 1052*, Materials Testing Institute, University of Stuttgart, 2006

[3] AICHER, S., HÖFFLIN, L., REINHARDT, H.W.: *Round holes in members made of glued laminated timber. Part 2: Load capacity and design.* (in German). In: *Bautechnik* Vol. 84.12 (2007), pp 867–800

[4] BLAß, H.J., STECK, G.: *Querzugverstärkungen von Holzbauteilen – Teil 1 und 2*. In: *Bauen mit Holz* 101 (1999), Heft 3, S. 42–46 und Heft 4, S. 44–49

[5] DANIELSSON, H.: *Strength tests of glulam beams with quadratic holes – Test report. English.* TVSM-7153. 2008.

[6] DANZER, M., DIETSCH, P., WINTER, S.: *Reinforcement of round holes in glulam beams arranged eccentrically or in groups*. In *CD-Rom Proceedings of the World Conference on Timber Engineering (WCTE 2016),* Vienna, Austria: Vienna University of Technology, Austria, 2016

[7] DANZER, M., DIETSCH, P., WINTER, S.: *Round holes in glulam beams arranged eccentrically or in groups*, In: *International Network on Timber Engineering Research — Meeting 50*. Kyoto, Japan, 2017

[8] DIN EN 1995-1-1-/NA: *National Annex – Nationally determined parameters – Eurocode 5: Design of timber structures – Part 1-1: General – Common rules and rules for buildings.* Berlin, Germany: Deutsches Institut für Normung e.V., 2013.

[9] EN 14358: *Timber Structures – Calculation and verification of characteristic values.* Brussels, Belgium: European Committee for Standardization, 2016

[10] EN 14454: *Timber Structures – Connectors – Requirements*, Brussels, Belgium: European Committee for Standardization, 2008

[11] FRECH, P., KOLB, H.: *Untersuchungen an durchbrochenen Bindern aus Brettschichtholz*, Test report H 30721, Materials Testing Institute, University of Stuttgart, 1974

[12] HÖFFLIN, L., AICHER, S.: *Design of rectangular holes in glulam beams*, In: *Otto-Graf-J.* 14 (2003), pp 211–229

[13] JOHANNESSON, B.: *Design problems for glulam beams with holes*, PhD thesis, Göteborg, Sweden: Div. of Steel and Timber structures, Chalmers University of Technology, 1983

[14] PENTALLA, V.: *Reiällinen liimapuupalkki*, Publication 33. Otaniemi: Division of Structural Engineering, Helsinki University of Technology, 1980

[15] TAPIA, C., AICHER, S.: *Improved design equations for the resultant tensile forces in glulam beams with holes*, In: *International Network on Timber Engineering Research — Meeting 50.* Kyoto, Japan, 2017